Concerted action of zinc and ProSAP/Shank in synaptogenesis and synapse maturation

Andreas M Grabrucker[1,2], Mary J Knight[3], Christian Proepper[1], Juergen Bockmann[1], Marisa Joubert[3], Magali Rowan[2], G Ulrich Nienhaus[4], Craig C Garner[2], Jim U Bowie[3], Michael R Kreutz[5], Eckart D Gundelfinger[6] and Tobias M Boeckers[1],*

[1]Institute of Anatomy and Cell Biology, University of Ulm, Ulm, Germany, [2]Department of Psychiatry and Behavioral Sciences, Stanford University, Stanford, CA, USA, [3]Department of Chemistry and Biochemistry, UC Los Angeles, CA, USA, [4]Institute of Applied Physics and Center for Functional Nanostructures (CFN), Karlsruhe Institute of Technology (KIT), Karlsruhe, Germany, [5]PG Neuroplasticity, Leibniz Institute for Neurobiology, Magdeburg, Germany and [6]Department of Neurochemistry/Molecular Biology, Leibniz Institute for Neurobiology, Magdeburg, Germany

Neuronal morphology and number of synapses is not static, but can change in response to a variety of factors, a process called synaptic plasticity. These structural and molecular changes are believed to represent the basis for learning and memory, thereby underling both the developmental and activity-dependent remodelling of excitatory synapses. Here, we report that Zn^{2+} ions, which are highly enriched within the postsynaptic density (PSD), are able to influence the recruitment of ProSAP/Shank proteins to PSDs in a family member-specific manner during the course of synaptogenesis and synapse maturation. Through selectively overexpressing each family member at excitatory postsynapses and comparing this to shRNA-mediated knockdown, we could demonstrate that only the overexpression of zinc-sensitive ProSAP1/Shank2 or ProSAP2/Shank3 leads to increased synapse density, although all of them cause a decrease upon knockdown. Furthermore, depletion of synaptic Zn^{2+} along with the knockdown of zinc-insensitive Shank1 causes the rapid disintegration of PSDs and the loss of several postsynaptic molecules including Homer1, PSD-95 and NMDA receptors. These findings lead to the model that the concerted action of ProSAP/Shank and Zn^{2+} is essential for the structural integrity of PSDs and moreover that it is an important element of synapse formation, maturation and structural plasticity.

*Corresponding author. Institute of Anatomy and Cell Biology, University of Ulm, Albert Einstein Allee 11, Ulm 89081, Germany. Tel.: +49 731 502 2331; Fax: +49 731 502 2317; E-mail: tobias.boeckers@uni-ulm.de

Introduction

During wiring of the central nervous system, synaptic contacts are constantly formed, stabilized or eliminated. For the establishment of new functional excitatory synapses, preformed scaffold protein complexes serve as predetermined postsynaptic sites (Gerrow *et al*, 2006). ProSAP/Shank proteins are observed at postsynaptic specializations early during synaptogenesis (Boeckers *et al*, 1999a; Petralia *et al*, 2005). The family of ProSAP/Shank proteins (also referred to as Synamon, CortBP, Spank and SSTRIP) consists of three members in mammals. They are efficiently targeted to synaptic sites (Sala *et al*, 2001; Boeckers *et al*, 2005) and attach receptor complexes to the local actin-based cytoskeleton within dendritic spines (Boeckers *et al*, 2002; Kim and Sheng, 2004; Rostaing *et al*, 2006). All ProSAP/Shank family members are expressed in the brain and are present at the postsynaptic density (PSD) of excitatory synapses (Boeckers *et al*, 1999b; Naisbitt *et al*, 1999); however, only Shank1 seems to be brain specific (Lim *et al*, 1999).

The appearance of ProSAP/Shank proteins at the PSD during neuronal development has been studied in the developing rat brain and in hippocampal cell culture (Boeckers *et al*, 1999a; Lim *et al*, 1999; Naisbitt *et al*, 1999). Localization data demonstrate that ProSAP1/Shank2 is one of the first protein components present in developing PSDs. It also becomes anchored to the subsynaptic cytoskeleton earlier than other known components of the PSD protein fraction, including SAP90/PSD-95 and NMDA receptors (Boeckers *et al*, 1999a). Expression of GFP-tagged ProSAP1/Shank2 and ProSAP2/Shank3 deletion constructs in hippocampal neurons reveals that the postsynaptic targeting of ProSAP1/Shank2 and ProSAP2/Shank3 is dependent on their SAM domains and the recruitment of ProSAP1/Shank2 and ProSAP2/Shank3 to the synapse is independent of their interaction with Homer (Boeckers *et al*, 2005). In contrast, the PDZ domain of Shank1 is mandatory for proper targeting to the synapse (Sala *et al*, 2001) and its localization at the PSD follows the formation of the SAP90/PSD-95-GKAP complexes (Naisbitt *et al*, 1999; Sheng and Kim, 2000). Overexpression of Shank1 alters spine morphology in transfected primary hippocampal neurons, leading to the enlargement of spine heads, an effect that depends on the PDZ domain and the Homer-binding site (Sala *et al*, 2001). Homer and ProSAP/Shank are among the most abundant scaffolding proteins in the PSD, working synergistically during the maturation of dendritic spines (Hayashi *et al*, 2009). The potency of ProSAP/Shank proteins to alter the morphology of the

postsynaptic compartment has also been shown by Roussignol et al (2005), who demonstrated that ProSAP2/Shank3 is essential for the maintenance of spines and synapses in hippocampal cultures. Moreover, overexpression of ProSAP2/Shank3 can induces spine formation in aspiny cerebellar neurons (Roussignol et al, 2005).

ProSAP/Shanks exhibit the capacity to form two-dimensional arrays by self-association via the SAM domain that are predicted to form a platform-like structure within dendritic spines (Baron et al, 2006). This association is regulated by Zn^{2+} ions, which might be released from the presynaptic terminal or from within dendritic spines leading to rapid changes within the PSD compartment (Gundelfinger et al, 2006). In the brain, free chelatable Zn^{2+} has been detected in presynaptic vesicles of glutamatergic terminals and Zn^{2+} released from the presynapse directly binds to and modulates glutamate receptors, thereby exerting significant effects on both acute synaptic transmission and long-term potentiation at hippocampal synapses (Li et al, 2001; Huang et al, 2008). Evidence has also been provided that Zn^{2+} ions are recruited into the molecular assemblies mediated by the SAM domains of ProSAP2/Shank3 and potentially ProSAP1/Shank2 (Baron et al, 2006; Gundelfinger et al, 2006) though how and if Zn^{2+} ions affect the molecular assembly of these proteins within dendritic spines remains unresolved. With > 4 nmol/mg protein, the Zn^{2+} content of purified PSDs is surprisingly high (Jan et al, 2002). Given the effect of Zn^{2+} on the packaging density of the ProSAP2/Shank3 2D arrays (Baron et al, 2006), we have proposed that chelatable Zn^{2+} might act to regulate postsynaptic dynamics and structural plasticity of excitatory synapses, (Gundelfinger et al, 2006).

Here, we explore the interplay between ProSAP/Shank family members and Zn^{2+} ions in living cells. Our results demonstrate that the zinc-sensitive isoforms, ProSAP1/Shank2 and ProSAP2/Shank3, are recruited to synapses prior to the zinc-insensitive isoform, Shank1. Moreover, changing the concentration of extracellular zinc was found to not only affect the synaptic levels of ProSAP1/Shank2 and ProSAP2/Shank3, but to dramatically influence the thickness of the PSD and the assembly of immature synapses. Furthermore, the zinc insensitivity of mature synapses was found to dependent on the synaptic expression of Shank1. These results lead to a new model, in which zinc through its actions on specific ProSAP/Shank family members regulate the initial formation and maintenance of nascent synapses as well as the stabilization, maturation and plasticity of mature excitatory synapses.

Results and discussion

Results

Previous studies have shown that ProSAP/Shank family members are localized to the PSDs of excitatory synapses (Boeckers et al, 1999a, b, 2002; Sala et al, 2001; Grabrucker et al, 2009a), yet their contribution to synapse formation and maturation are not well understood. In an initial set of experiments, we examined whether gain (overexpression of GFP-tagged ProSAP/Shank) or loss of function (shRNA-mediated knockdown) influenced synapse number in hippocampal neuron grown for 9 days in vitro (DIV). When neurons were transfected at DIV 6 and examined at DIV 9 GFP-tagged ProSAP1/Shank2 and ProSAP2/Shank3 effi-

ciently colocalize with the synaptic markers Bassoon and Homer (Figure 1A), while GFP-tagged Shank1 exhibited a limited synaptic localization (Figure 1A). An analysis of synaptic density/unit length of dendrite revealed that GFP-tagged ProSAP1/Shank2 and ProSAP2/Shank3 overexpression caused a significant increase in the number of synapses, while GFP-Shank1 overexpression had little effect (Figure 1B). Consistent with a role of these PSD proteins in synapse formation, knockdown of ProSAP/Shank proteins causes a significant reduction in synapse density (Figure 1B; Supplementary Figure S1).

In a previous study, we identified the C-terminal SAM domain as a region critical for the postsynaptic localization of ProSAP1/Shank2 and ProSAP2/Shank3 (Boeckers et al, 2005; Grabrucker et al, 2009b). Intriguingly, Shank1, though it has a SAM domain, utilizes its PDZ domain for its synaptic localization (Sala et al, 2001). In the case of ProSAP1/Shank2 and ProSAP2/Shank3, the SAM domain is predicted to facilitate the oligomerization of these isoforms in a Zn^{2+}-dependent manner and possibly the assembly of these ProSAP/Shank isoforms into a two-dimensional lattice within dendritic spines (Baron et al, 2006). We were thus interested to explore whether their overexpression and/or zinc binding affects their synaptic localization and/or synapse assembly. In initial experiments, the GFP-tagged SAM domains of ProSAP1/Shank2 and ProSAP2/Shank3 were found to reliably become synaptically localized when overexpressed in DIV 9 neurons, yet had no significant effect on synapse number (Figure 1B). Similar to full-length GFP-Shank1, the SAM domain of Shank1 only poorly localized to synapses at 9 DIV and had no effect on synapse number (Figure 1A and B). Interestingly, although full-length Shank1 exhibits a microtubular-like pattern, in immature neurons 9 DIV (Figure 1A), it becomes synaptic in older cultures (Supplementary Figure S1B and C), indicating that the postsynaptic localization of Shank1 is tightly controlled limiting its influence to mature synapses. The overexpression in young neurons might lead to an accumulation of protein outside synaptic compartments, resulting in a shift of Shank1 localization to other interaction partners.

In the next set of experiments, we were keen to investigate the role of Zn^{2+} ions on SAM domain function and a possible influence on synapse formation and maturation. For these experiments, we took advantage of a dye (Zinquin) that fluoresces when it binds zinc (Coyle et al, 1994; Fahrni and O'Halloran, 1999) (Supplementary Figure S2A). To test the hypothesis that ProSAP/Shank SAM domains bind Zn^{2+} in vivo, transfected HeLa cells cultured in media supplemented with Zn^{2+} (30 μM) were stained with Zinquin. In untransfected HeLa cells, Zinquin staining labels small naturally occurring zinc-positive clusters. The application of $ZnCl_2$ to the medium strongly enhances the intracellular Zinquin signals (Supplementary Figure S2B). Zn^{2+} binds to Zinquin by complexing with either one or two nitrogen atoms to form complexes in a ratio of 1:1 (Zn^{2+}:Zinquin) or 1:2. However, a wide range of free Zn^{2+} concentrations have been estimated in studies with Zinquin, ranging from femtomolar to micromolar concentrations, thereby raising the question of what Zinquin is measuring. Strikingly, Coyle et al (1994) showed in hepatocyte homogenates that Zinquin fluoresced with protein-bound Zn^{2+} across a broad range of molecular weights. There was no evidence that Zinquin removed
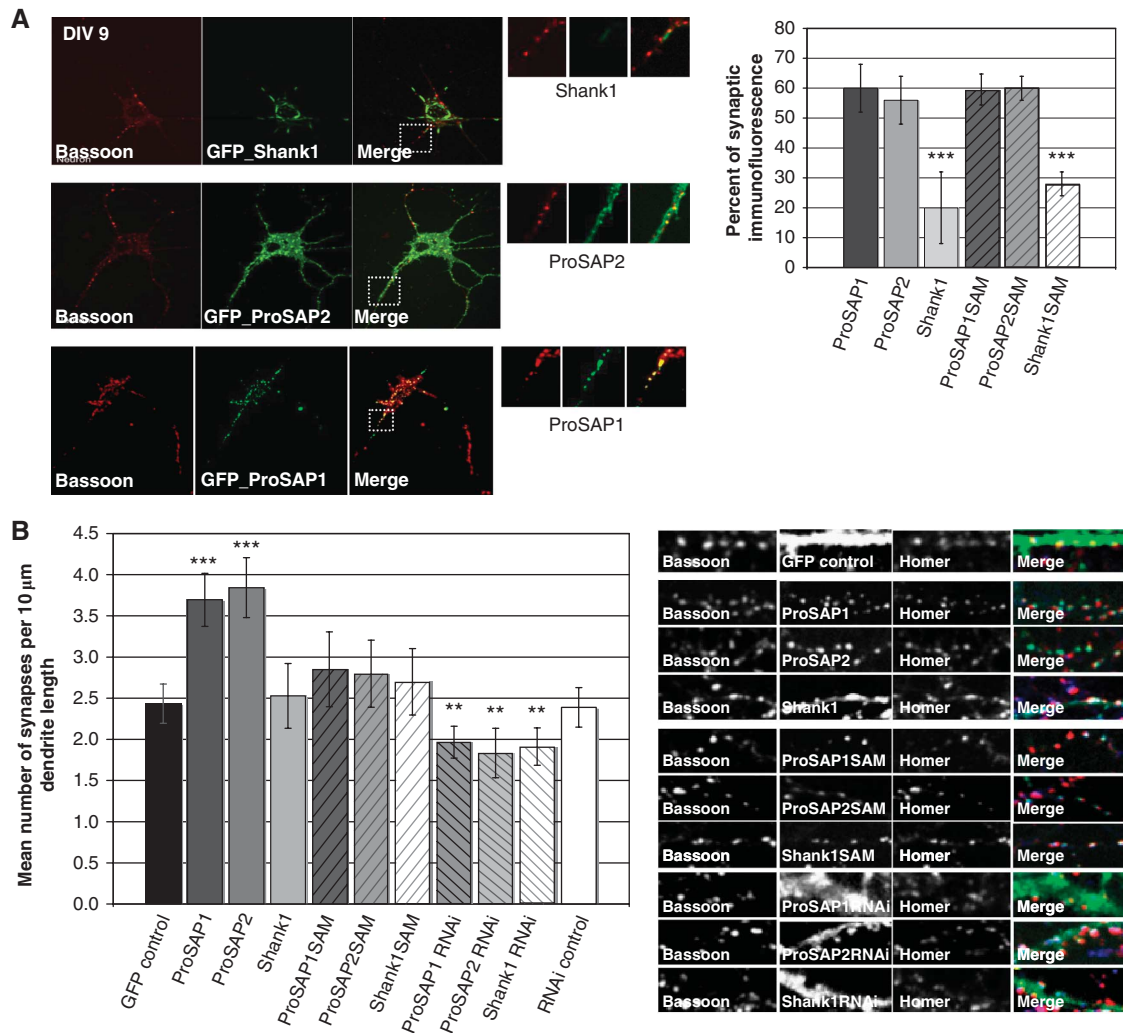
Figure 1 In young neurons, overexpressed ProSAP1/Shank2 and ProSAP2/Shank3, but not Shank1, increase synapse density and localize to synaptic contact sites. (**A**) Hippocampal neurons were transfected at 6 DIV with full-length and C-terminal ProSAP/Shank constructs and cells were fixed at 9 DIV. ProSAP1/Shank2 and ProSAP2/Shank3 localize at synapses in contrast to Shank1. The percentage of punctate GFP signals colocalizing with Homer/Bassoon signals was assessed. Shank1 shows significantly less localization to synapses. Although the C-terminal Shank1 construct shows a punctate distribution in contrast to full-length Shank1, the Shank1 C-terminal clusters are mostly non-synaptic. (**B**) The number of synapses defined by Homer/Bassoon colocalizing signals was measured per 10 μm dendrite length in ProSAP/Shank full-length and C-terminal constructs overexpressing hippocampal neurons. ProSAP1/Shank2 and ProSAP2/Shank3 overexpression from DIV 6 to DIV 9 significantly increases the number of synapses. Shank1 overexpression shows no increase. ProSAP/Shank C-terminal constructs did not show any significant alteration. The knockdown of each ProSAP/Shank member causes a significant reduction in synapse density. Images show hippocampal neurons transfected with GFP expressing constructs and stained for Homer-Alexa 647 (coloured blue in 'Merged' pictures) and Bassoon-Alexa-568 (coloured red in 'Merged' pictures). $*P = 0.5$; $**P = 0.01$; $***P = 0.001$.

Zn^{2+} from high molecular weight proteins. Taken together, these data indicate that Zinquin sequesters zinc that is labile or loosely bound to proteins, using ill-defined ligand-exchange mechanisms (Coyle *et al*, 1994; Fahrni and O'Halloran, 1999). In Hela cells transfected with GFP-tagged ProSAP1/Shank2 or ProSAP2/Shank3, we observed the appearance of large intracellular clusters, which nicely colocalize with Zinquin fluorescent puncta (Figure 2A and C). A high degree of colocalization with Zinquin fluorescent puncta was also seen in cells expressing the C-terminal SAM domain of ProSAP1/Shank2 or ProSAP2/Shank3 tagged with GFP (Figure 2A and C). No colocalization of zinc dye with GFP was observed upon transfection of HeLa cells with other cluster-forming PSD molecules, such as Abi-1 (Supplementary Figure S2C). Similarly, expression of the Shank1-SAM domain, constructs lacking the ProSAP1/

Shank2- or ProSAP2/Shank3-SAM domains, or constructs harbouring a mutation in the Zn^{2+}-binding site within the ProSAP2/Shank3-SAM domain do not display any overlap with Zinquin fluorescent puncta (Figure 2A). Intriguingly, the addition of 300 μM $ZnCl_2$ leads to an increase in cluster size of GFP-ProSAP2/Shank3 in HeLa cells (Supplementary Figure S2D). In contrast, the localization pattern of Shank1 is not affected by the addition of 300 μM $ZnCl_2$ (Supplementary Figure S2D). Together, these data suggest that zinc levels may control the oligomerization state of specific ProSAP/Shank family members via the self-association of isoform-specific SAM domains. To more directly test this hypothesis, we created and purified fusion proteins between maltose-binding protein (MBP) and the SAM domains of ProSAP2/Shank3 or Shank1. When MBP-ProSAP2/Shank3(SAM) was incubated with an equimolar amount of

zinc, the majority of the protein precipitates (data not shown). In contrast, when MBP-Shank1(SAM) protein is incubated with zinc, only a minor fraction of the protein precipitates (data not shown). Note, in previous work, we found that the Zn^{2+}-induced precipitate of ProSAP2/Shank3(SAM) contains a large fraction of SAM-organized sheets (Baron et al, 2006). To confirm that Zn^{2+} was changing the oligomerization state, the supernatant of
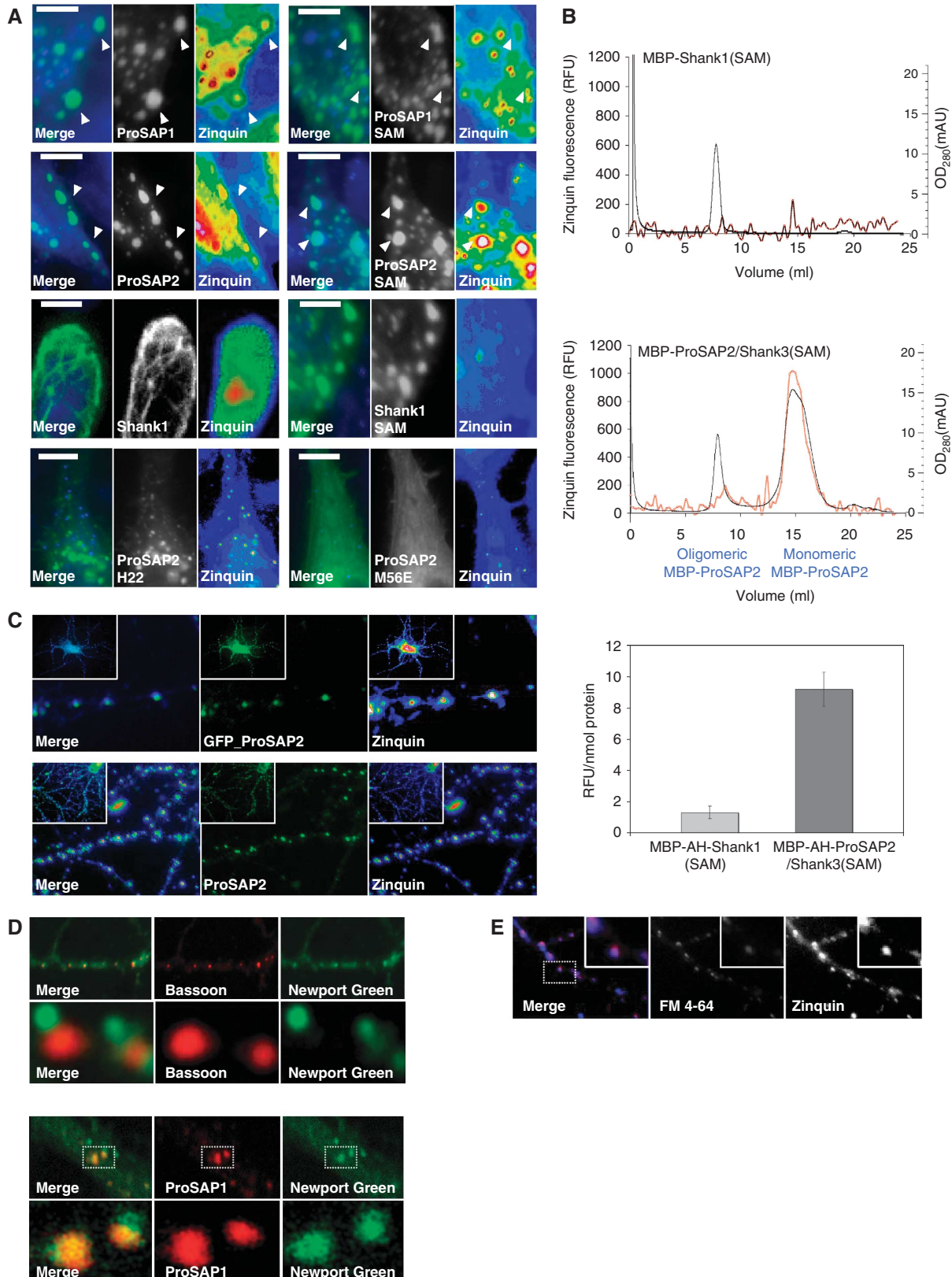
zinc-treated samples of MBP-ProSAP2/Shank3(SAM) and MBP-Shank1(SAM) were loaded onto a gel-filtration column and individual fractions assayed with Zinquin. A significant Zinquin fluorescence signal was detected in fractions that contain both MBP-ProSAP2/Shank3(SAM) monomers and polymers, but no signal was detected in MBP-Shank1(SAM) fractions (Figure 2B). As a further measure that the SAM domain of ProSAP2/Shank3 binds Zn^{2+}, we assessed Zinquin fluorescence in the zinc-induced precipitates of ProSAP/Shank proteins. While the purified MBP-ProSAP2/Shank3(SAM) samples produced a strong fluorescence signal, the MBP-Shank1(SAM) samples only yielded a Zinquin signal of roughly 8% of the ProSAP2/Shank3 signal (Figure 2B). These results demonstrate that ProSAP2/Shank3-SAM domains are able to bind bivalent Zn^{2+} ions in vitro while Shank1 binds much lower levels of Zn^{2+}. This is consistent with our prediction that amino-acid exchanges in the sheet interface of the Shank1 SAM domain allows it to form zinc-independent sheets (Baron et al, 2006; Gundelfinger et al, 2006). Intriguingly, the Zn^{2+}-binding sites of ProSAP1/Shank2 and ProSAP2/Shank3, however, are completely conserved (Boeckers et al, 2005) and binding of other divalent metal ions is nearly absent (Supplementary Figure S2E).

One prediction of these biochemical studies is that ProSAP/Shank-positive dendritic spines should also contain Zn^{2+}. To test this concept, we overexpressed GFP-ProSAP2/Shank3 in cultured hippocampal neurons and stained these neurons with Zinquin. Figure 2C reveals a striking colocalziation of dendritic GFP-ProSAP2/Shank3 clusters and Zinquin fluorescent puncta. Cultures stained with antibodies against ProSAP1/Shank2 and ProSAP2/Shank3 revealed that Zinquin or Newport Green puncta also colocalized with endogenous ProSAP2/Shank3 and ProSAP1/Shank2 postsynaptic clusters, respectively (Figure 2C and D). Previous studies on zinc in neurons have found that it is particularly enriched in presynaptic nerve terminal especially those expressing the zinc transporter ZnT3 (Palmiter et al, 1996; Wenzel et al, 1997). To assess whether the detected synaptic zinc was presynaptic or postsynaptic, we compared the spatial localization of Zinquin fluorescent puncta with endogenous ProSAP1/Shank2 and Bassoon, a presynaptic active zone protein, or presynaptic boutons loaded with the styryl dye FM4-64 (Figure 2D and E). The results show that the detected Zn^{2+} signal colocalizes with postsynaptic markers. Note, that Newport Green (a second zinc-binding dye) was used to confirm our data with Zinquin that postsynaptic structures contain zinc.

A critical question raised by these studies is whether Zn^{2+} levels in neurons affect the synaptic distribution of zinc-binding isoforms of ProSAP/Shank. This question was initially addressed by acutely removing Zn^{2+} from cultured hippocampal neurons by the application of a more potent chelator than Zinquin such as TPEN. Here, we found that 10 μM TPEN caused a translocation of ProSAP1/Shank2 and ProSAP2/Shank3 proteins from PSDs into the dendritic compartment within a few minutes (Figure 3A and B; Supplementary Figure S3A). The localization of other molecular PSD components including Shank1 and glutamate receptors as well as the overall number of PSDs remained unchanged. Additionally, hippocampal neuronal cultures were treated with TPEN at DIV 14 and protein fractionation was performed. Consistent with the previous results, the amount of ProSAP1/Shank2 and ProSAP2/Shank3, but not Shank1 increases in the S2 protein fraction after zinc depletion compared with untreated neurons (Figure 3B). This shift is further emphasized by the fact that the ProSAP2/Shank3 protein can be washed out with Triton X-100 from the dendritic compartment to a higher degree in zinc-depleted neurons (Supplementary Figure S3A). Importantly, the effect of zinc depletion on the localization of ProSAP2/Shank3 depends upon the applied concentration of the zinc chelators, but leaves the staining of the presynaptic marker protein Bassoon unchanged. These effects of zinc depletion are reversible by the supplementation of Zn^{2+} ions, but not by Ca^{2+} or Mg^{2+} (Supplementary Figure S3).

One hallmark of excitatory synapses is the presence of a pronounced PSD that is thought to arise due to a high concentration of postsynaptic scaffold proteins (Gray, 1959). Given the striking effects of TPEN and $ZnCl_2$ on the postsynaptic levels of ProSAP/Shank proteins, we examined the ultrastructural organization of synapses following these manipulations. Intriguingly, the application of 10 μM TPEN led to a significant reduction of PSD thickness and area, while the application of 300 μM Zn^{2+} caused in a significant increase in PSD thickness (Figure 3C). Quantifying synapse morphology using semiquantitative criteria 'normal PSD', 'strong PSD' or 'without PSD' indicates that the percentage of synaptic contacts without a PSD is higher in the zinc chelator groups (TPEN, CaEDTA), while $ZnCl_2$ treatment leads to the increased appearance of 'strong' PSDs (Figure 3D). These data indicate that altering zinc levels can have dramatic effects on PSDs by modulating the postsynaptic levels of Zn^{2+}-sensitive ProSAP/Shank isoforms.

Intriguingly, the effect of Zn^{2+} chelators on postsynaptic morphology was particularly pronounced in young neurons (DIV 7). This was explored by staining cultured neurons with antibodies against Homer1 to mark excitatory postsynapses and Bassoon as a presynaptic marker. For evaluation, fluorescent puncta along dendrites were counted and the mean number of monofluorescent ('Bassoon only') and double-

Figure 2 The SAM domains of ProSAP1/Shank2 and of ProSAP2/Shank3 specifically bind zinc ions. (**A**) Full-length GFP-ProSAP1/Shank2, ProSAP2/Shank3 or their C-terminal SAM domains colocalize with Zn^{2+} stained with Zinquin (arrowheads) in HeLa cells. GFP-Shank1 or its C-terminal SAM domain do not colocalize with Zinquin. Mutations of the ProSAP2/Shank3 SAM domain within the zinc-binding site (H22A) or the site of oligomerization (M56E) (Baron et al, 2006) abolish Zinquin colocalization. (**B**) Gel filtration of purified maltose-binding protein (MBP)-Shank1 (upper panel) and MBP-ProSAP2/Shank3 (middle panel) after zinc preincubation (solid black line). The plots are overlayed with Zinquin fluorescence profile (red lines, open circles). Quantification of the Zinquin fluorescence signals per nmole of zinc-precipitated MBP-AH-Shank1 and MBP-AH-ProSAP2/Shank3 protein (lower panel). (**C**) Transfection of ProSAP2/Shank3-GFP shows that EGFP signals cocluster with the fluorescence zinc dye Zinquin in hippocampal neurons in culture. Similarly, Zinquin signals colocalize with endogenous ProSAP2/Shank3 staining. (**D**) Immunolabelling of excitatory synapses of cultured hippocampal neurons (14 DIV). The zinc signal (Newport Green) colocalizes with the PSD protein ProSAP1/Shank2 and is juxtaposed to the presynaptic marker Bassoon. (**E**) The postsynaptic enrichment of zinc can be visualized in living cells, using the FM dye 4–64 that labels recycling presynaptic vesicles and Zinquin.

fluorescent ('Bassoon and Homer') signals were compared under control and zinc-depleted conditions. Here, we observed a complete loss of Homer1 immunoreactivity, in about 40% of synapses, within a short time after treatment, with little if any effect on Bassoon fluorescence (Figure 4A and B). Importantly, the overall number of presynaptic contact sites remains unchanged. These data suggest that zinc depletion is causing a selective disassembly of the PSD scaffold. Surprisingly, at later stages of synaptic maturation (DIV 14), the reduction of the postsynaptic Homer1 signal is not observed (Figure 4B). This latter observation suggests that PSDs undergo a developmental change in their molecular composition. To explore whether this is due to changes in the synaptic expression patterns of ProSAP/Shank family members, cultures at different stages were fixed and stained with

antibodies against Bassoon and different ProSAP/Shank isoforms at DIV 7, 10, 14 and 21. As shown previously (Boeckers et al, 1999a), ProSAP1/Shank2 is the first family member to appear at PSDs, whereas the recruitment of ProSAP2/Shank3 and Shank1 occurs at later times (Figure 5A). At any given stage, it was possible to identify postsynaptic specializations containing either ProSAP1/Shank2 only, or ProSAP1/Shank2 and ProSAP2/Shank3, or all three family members (Figure 5A). During the early development of synaptic contacts (DIV 7), two thirds of all PSDs do not contain any Shank1. Based on the observations that the Shank1 SAM domain does not effectively bind Zn^{2+} ions (Figure 2B), that synaptic targeting does not depend on its SAM domain (Naisbitt et al, 1999), and that most Shank1 isoforms do not contain a SAM domain (Sheng and Kim, 2000), we postulated that the absence or presence of Shank1 might confer 'Zn^{2+} sensitive' or 'insensitive', respectively. Based on this hypothesis, one would expect that (i) lowering of Zn^{2+} concentrations in parallel with Shank1 depletion should lead to a drastic reduction of PSDs in mature synapses and (ii) overexpression of the synaptic Shank1 and PSD-95/GKAP at early stages of synaptogenesis should stabilize PSDs. To test the first part of this hypothesis, we transfected DIV 11 neurons with a Shank1-RNAi construct, then applied TPEN to the cultures at DIV 14 for 20 min before fixation. The cells were then stained for the postsynaptic scaffolding proteins Homer1 or PSD-95 or the NR1 subunits of NMDA receptor. Under these conditions, Homer1 was often not found opposite Bassoon-positive presynaptic sites at 14 DIV. Moreover, PSD-95 and NMDA receptors were significantly reduced by 25–30% within this very short time period (Figure 5B). The reduction of these postsynaptic proteins was not observed when TPEN was applied to neurons transfected with control vectors (pSUPER) or when Shank1-RNAi-transfected neurons without TPEN treatment were analysed. Overexpression of an RNAi-resistant Shank1 construct containing conservative mutations within the RNAi target sequence completely rescued the effect of Shank1-RNAi knockdown and Zn^{2+}
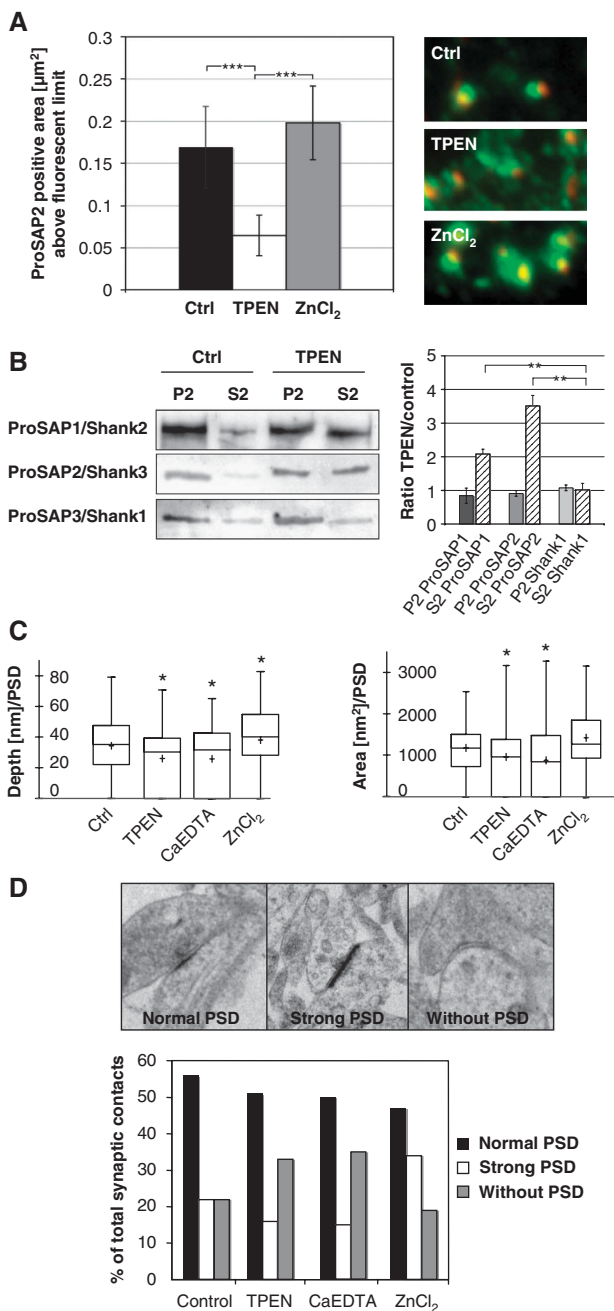
Figure 3 Zinc can rapidly alter the morphology of synaptic contacts and the attachment of ProSAP1/Shank2 and ProSAP2/Shank3 at PSDs. (A) A 20-min application of the zinc chelator TPEN results in the loss of defined ProSAP2/Shank3 dots (green) adjacent to presynaptic specializations as marked by Bassoon immunoreactivity (red). Measurement of the ProSAP2/Shank3-positive area above a present fluorescence limit illustrates the significant reduction within the TPEN group (control 0.17 ± 0.055 versus 0.06 ± 0.03) and a slight enlargement upon $ZnCl_2$ treatment (0.2 ± 0.05). Altogether, >500 synapses were measured for each condition and the results were corrected for inhibitory synapses, which are positive for Bassoon but a priori negative for ProSAP/Shanks. The mean number of inhibitory synapses per cell was assessed via Gepyhrin and Bassoon staining and amounted to 23.1 ± 1.33%. (B) Western blot analysis of neuronal P2 and S2 fractions without and with short TPEN treatment shows that the zinc-binding proteins ProSAP1/Shank2 and ProSAP2/Shank3 are shifted towards the soluble fraction while the Shank1 signal stays unchanged upon TPEN application. (C) Ultrastructural analysis of PSD depth and area by electron microscopy shows a significant reduction of both parameters for TPEN and CaEDTA application and a slight enlargement in the $ZnCl_2$ group. (D) The ultrastructural analysis of synaptic contacts according to the semiquantitative criteria 'normal PSD', 'strong PSD' or 'without PSD' indicates that the percentage of synaptic contacts without a PSD is higher in the zinc chelator groups (TPEN, CaEDTA), while $ZnCl_2$ treatment leads to the increased appearance of 'strong' PSDs. *$P = 0.5$; **$P = 0.01$; ***$P = 0.001$.
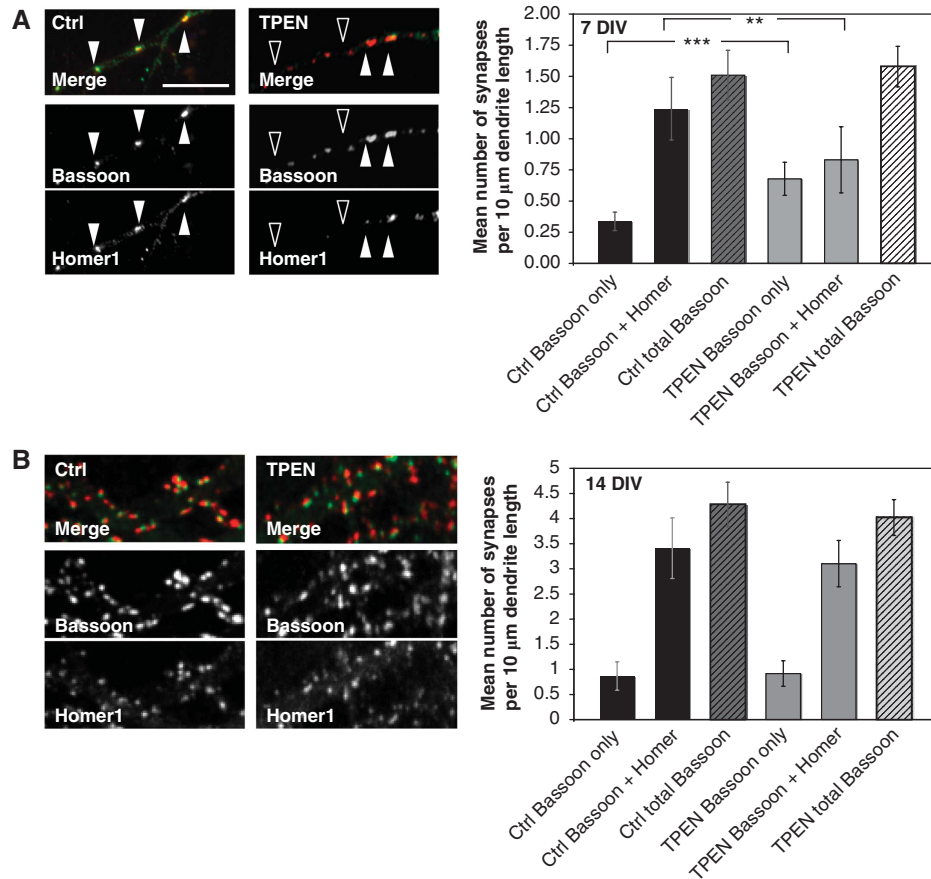
Figure 4 Loss of the postsynaptic marker molecule Homer1 upon TPEN treatment. (**A**) Application of TPEN to DIV 7 neurons results in a loss of about 40% of Homer1 signals colocalizing with the presynaptic marker Bassoon. The overall number of presynaptic contact sites remains unchanged. (**B**) At DIV 14, the reduction of the postsynaptic Homer1 signal is not observed. The cells were stained using Homer1 antibodies to mark excitatory postsynapses and Bassoon as a presynaptic marker protein. For evaluation, fluorescent puncta along dendrites within the field of view were counted and the mean number of monofluorescent ('Bassoon only') and double-fluorescent ('Bassoon and Homer') signals were compared under control and zinc-depleted conditions. $*P = 0.5$; $**P = 0.01$; $***P = 0.001$.

depletion (Figure 5B). An analysis of changes in spine morphology showed that neither the downregulation of Shank1 nor zinc depletion alone had any significant effect on spine morphology. However, there was a trend towards more 'filopodia-like' synapses in Shank1 knockdown cells. These latter findings parallel those reported on Shank1 knockout mice (Hung *et al*, 2008). In our experiments, Shank1 knockdown together with zinc depletion also reduced the number of 'mushroom/stubby' synapses and leads to a shift towards 'filopodia-like' and 'thin' synapses (Supplementary Figure S4). This shift may be due to a decrease in the spine size of 'mushroom-like' synapses, thereby increasing the number of 'thin' spines. Finally, to assess whether Shank1 could convert immature synapses to Zn^{2+}-insensitive synapses, we transfected young neurons at DIV 7 with GKAP, PSD-95 and Shank1 and then applied the Zn^{2+} chelator TPEN. As reported earlier, triple transfection of these proteins leads to synaptic clustering of Shank1 in young neurons (Romorini *et al*, 2004) (data not shown). Immunocytochemistry for endogenous Homer1 and Bassoon was performed on untreated cells and the number of Bassoon only and Bassoon and Homer1 positive signals was counted and compared with zinc-depleted cells. There is no significant difference between Zn^{2+}-depleted (Zn−) and untreated neurons in triple-transfected cells (Figure 5C),

indicating that Shank1 is a key PSD maturation molecule that reduces the zinc sensitivity of immature synapses.

Conclusions

Synapse formation, maturation and plasticity are essential aspects of neural development guiding the appropriate wiring and functioning of neuronal circuits as well as the acquisition, storage, retrieval and processing of sensory information, thus dictating our behaviour. Abnormalities in the properties of synapses can have profound effects on development, learning and memory mechanisms, behaviour and disease (Bailey and Kandel, 1993; Horner, 1993; Harris and Kater, 1994). It is thus perhaps not surprising that there is a growing number of development, psychiatric and neurodegenerative disorders that are associated with mutations in synaptic proteins. With regard to excitatory synaptic function, mutations in the ProSAP/Shank family are perhaps some of the most exciting given their link to autism spectrum disorders (Durand *et al*, 2007; Berkel *et al*, 2010) and Alzheimer's disease (Gong *et al*, 2009; Roselli *et al*, 2009; Pham *et al*, 2010). Yet how they mechanistically alter the function of excitatory synapses, circuit function and behaviour is poorly understood. On many levels, ProSAP/Shank family members appear to function as master organizers of the PSD during early development given their ability to physically interact
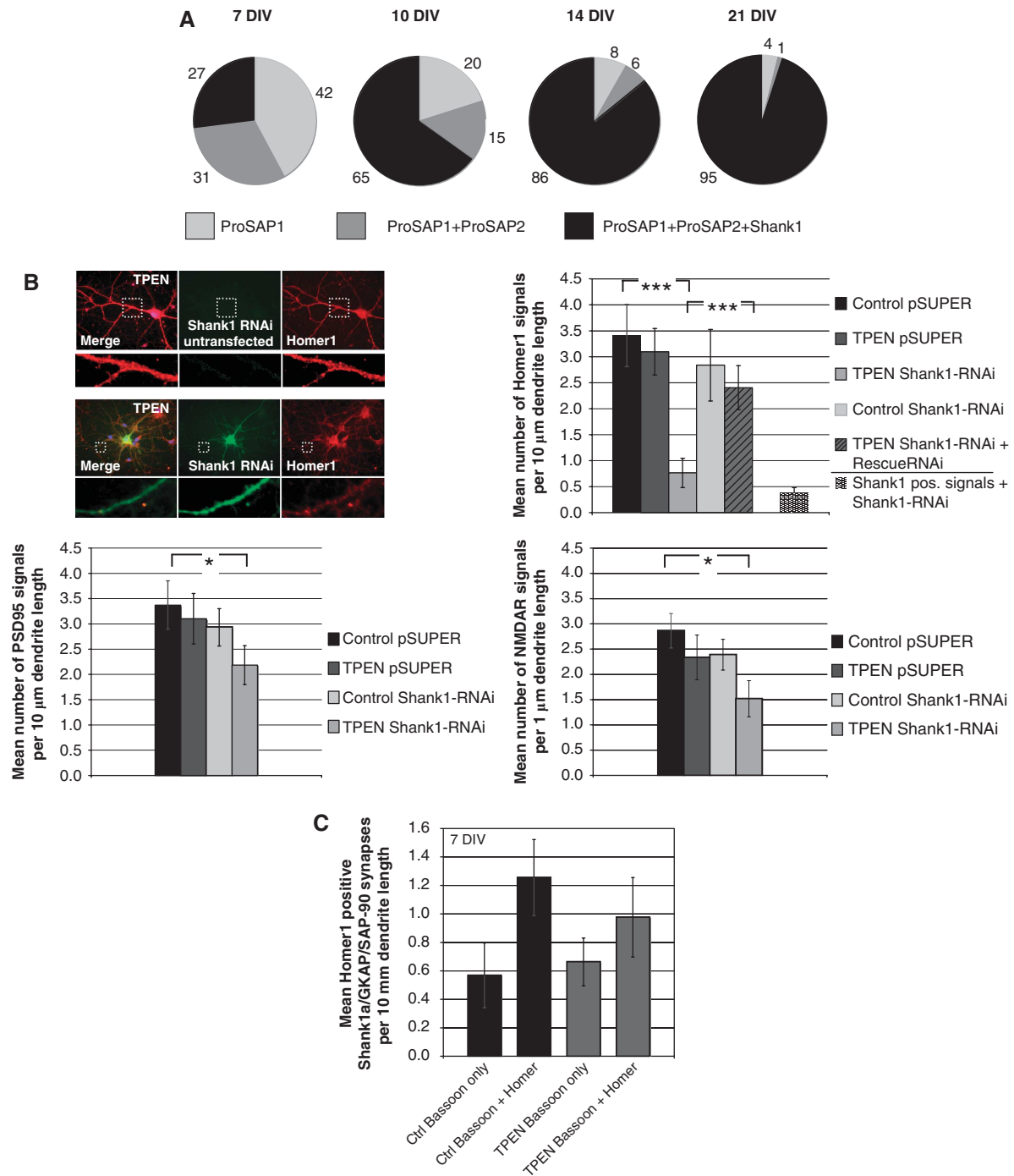
Figure 5 Shank1 and zinc depletion significantly influence the number of synapses depending on synapse maturity. (**A**) ProSAP/Shank family members are recruited consecutively to postsynaptic sites. Only postsynaptic specializations containing either ProSAP1/Shank2 only, or ProSAP1/Shank2 and ProSAP2/Shank3, or all three family members are found (percentages of these PSD types are indicated at different stages of development in primary culture). During early development of synaptic contacts (DIV 7), two thirds of all PSDs do not contain any Shank1. During further development, the fraction of triply positive postsynapses steeply increases, and at DIV 21 >95% of all synapses are labelled by antibodies against all three ProSAP/Shank family members. (**B**) The specific downregulation of Shank1 by transfection of Shank1-RNAi significantly reduced the Homer1-positive signal after TPEN treatment. This reduction was not seen in untransfected neurons, without TPEN treatment or upon cotransfection of a Shank1-RNAi-resistant protein to rescue the loss of endogenous protein. Staining against Shank1 in Shank1-RNAi-transfected neurons indicates the overall reduction of Shank1-positive signals to about 12% in comparison to controls. Additionally, Shank1 downregulation and TPEN treatment (20 min) significantly reduced the number of PSD-95 and NMDAR-positive PSDs to about 60%. The reduction of both postsynaptic proteins was not observed when TPEN was applied to vector control transfected cells or Shank1-RNAi-transfected neurons without TPEN treatment. The cells were stained using Homer1, PSD-95 or NMDAR1 antibodies. For evaluation, fluorescent puncta along primary and secondary dendrites within the field of view were counted and the mean number of fluorescent signals was compared under the different conditions. (**C**) Shank1 stabilizes young synapses (7 DIV). Immunocytochemistry for endogenous Homer1 and Bassoon was performed on untreated cells and the number of Bassoon only and Bassoon and Homer1 positive signals was counted and compared with zinc-depleted cells. All cells were triply transfected with Shank1a-GFP, GKAP and PSD-95-Myc. There is no significant difference between Zn^{2+}-depleted (Zn−) and untreated neurons. For evaluation, fluorescent puncta along dendrites within the field of view were counted and the mean number of monofluorescent ('Bassoon only') and double-fluorescent ('Bassoon and Homer') signals was compared. $*P = 0.5$; $**P = 0.01$; $***P = 0.001$.

with all of the major classes of postsynaptic proteins including other scaffold proteins, ligand and voltage-gated ion channels, metabotropic receptors and the actin cytoskeleton of dendritic spines (Boeckers *et al*, 2002). A major open question is why autism-associated mutations have only been identified in ProSAP1/Shank2 and ProSAP2/Shank3 but not Shank1 (Durand *et al*, 2007; Berkel *et al*, 2010). Presumably, this is due to either a difference in the temporal expression of these proteins or their intrinsic properties.

A relationship between zinc deficiency and learning behaviour has been reported in laboratory animals such as rats and rhesus monkeys (Golub *et al*, 1995). Zinc deficiency during early development elicits critical and irrecoverable impairment of learning and memory (Takeda, 2000). In the current study, we have compared the development expression pattern and the contribution of Zn^{2+} ions on the recruitment and dynamics of the three primary ProSAP/Shank isoforms, ProSAP1/Shank2, ProSAP2/Shank3 and Shank1. Our results show that immature synapses exhibit a striking sensitivity to extracellular levels of Zn^{2+} ions that is not shared by mature synapses. Moreover, our data show that this sensitivity is intimately linked to the differential expression and selective binding of Zn^{2+} ions to ProSAP1/Shank2, ProSAP2/Shank3 but not Shank1. These data indicate that ProSAP/Shank family members are key regulators in the formation, stability and maturation of excitatory synapses and that the zinc-binding properties of ProSAP1/Shank2 and ProSAP2/Shank3 provide immature excitatory synapses with unique properties that both facilitate synaptogenesis, yet make impart a vulnerability to dysregulation and disease.

Our analysis of ProSAP/Shank family members reveal that their levels at the PSD are tightly regulated via Zn^{2+} ions in an isoform-specific way, such that ProSAP1/Shank2 and ProSAP2/Shank3 are sensitive to Zn^{2+} ions via their SAM domains, while Shank1 is Zn^{2+} insensitive. Given that Shank1 is the last ProSAP/Shank family member to appear at newly forming synapses, this argues for a role of Shank1 in synapse maturation rather than synaptogenesis. In contrast, ProSAP1/Shank2 and ProSAP2/Shank3 appear early in forming synapses, leading to a time window in synaptogenesis, where the postsynaptic ProSAP/Shank scaffold is very plastic and dependent on synaptic activity accompanied by Zn^{2+} influx and where only sufficient strengthening of the ProSAP1/ProSAP2 scaffold will finally lead to the clustering of Shank1 and maturation of the synaptic contacts. Overexpression of Shank1 not only increases synapse maturation, but additionally alters the spine morphology, shifting to a mushroom-like appearance (Sala *et al*, 2001). Our experiments show, similar to overexpression of Shank1 later in development (Sala *et al*, 2001), that spine number was not changed. In contrast, shRNA-mediated knockdown of Shank1 caused a reduction in spine density. These results support data by Sala *et al* (2001), speculating that the level of endogenous Shank1 protein is limiting during synapse maturation but that Shank1 levels are not a limiting factor during synapse formation. Furthermore, it supports the model that normal spines may need to mature and grow to a certain size before being stabilized by Shank1 (Sala *et al*, 2001). The knockdown of Shank1 possibly results in a higher proportion of unstable spines that may be degraded, leading to a reduction in spine density. Therefore, one may hypothesize that Shank1 has a critical role in the consolidation of

novel synaptic contacts, and thus possibly in memory formation as a behavioural correlate. Interestingly, Shank1-deficient mice display enhanced performance in a spatial learning task but have impaired long-term memory retention in this task (Hung *et al*, 2008). These results affirm the role of Shank1 for the maturation of synaptic structures rather than their *de novo* generation *in vivo*.

Tetrameric Homer crosslinks the multimeric ProSAP/Shank platforms, resulting in the formation of a polymerized matrix structure (Hayashi *et al*, 2009). Since such a complex does not have any theoretical limit in size, the addition of ProSAP1/Shank2 and ProSAP2/Shank3 in an activity/Zn^{2+} dependent manner provides a mechanism for enhancing Shank1 clustering and synaptic strength in mature and Shank1 stabilized synapses. Conceptually, the formation of ProSAP/Shank platforms is predicted to direct the further recruitment of additional postsynaptic proteins such as Abp1 and Homer influencing not only the properties of the PSD and dendritic spines, but also transsynaptic adhesion and signalling and the maturation and properties of presynaptic boutons (Gerrow *et al*, 2006). The disruption of ProSAP/Shank platforms is thus predicted to lead to an impairment of excitatory synapse function and maturation. Since ProSAP/Shank proteins are not found at inhibitory synapses, this might lead to an imbalance of excitation and inhibition within neuronal circuits. On a neuronal level, the amount and distribution of excitatory and inhibitory synapses along a single cell has a significant impact on the integration of synaptic inputs and the output from these neurons. This influences synaptic plasticity, for instance through alteration of long-term potentiation (Wigstrom and Gustafsson, 1983). It is well known that an imbalance of excitation and inhibition may underlie several neurological diseases, such as autism (Rubenstein and Merzenich, 2003), Tourette's syndrome (Singer and Minzer, 2003), schizophrenia (Wassef *et al*, 2003) and Down's syndrome (Fernandez *et al*, 2007). Interestingly, a mutation associated with schizophrenia was reported for ProSAP2/Shank3 (Gauthier *et al*, 2010). These data imply that these zinc-sensitive isoforms endow excitatory synapses with critical functions that also make them sensitive to genetic insults and disease. At present, our data suggest that these two isoforms are critical for the assembly and stability of immature synapses, while the zinc-insensitive isofrom Shank1 facilitates synaptic maturation.

The contribution of Zn^{2+} on ProSAP/Shank family members is impressively illustrated when Zn^{2+} and Shank1 are depleted. This constellation putatively resembles a 'triple-deficiency' situation for ProSAP/Shank. The loss of all ProSAP/Shank family members and thus the destabilization of the ProSAP/Shank scaffold within the PSD results in a reduced size and partial loss of PSDs of excitatory synapses within 15–20 min and is accompanied by a decrease in the levels of interaction partners such as Homer as well as other PSD proteins, including PSD-95 and NMDAR. Zn^{2+} has been shown to be highly concentrated in PSDs of excitatory synapses in the central nervous system and to be able to significantly modulate the structure of the protein meshwork underneath the postsynaptic membrane within a few minutes. Zn^{2+}-level dependent induced changes in ProSAP1/Shank2 and ProSAP2/Shank3 might correlate with the local turnover of these proteins at synapses. Indeed, Bresler *et al* (2004) found that in young neurons, the turnover

of ProSAP1/Shank2 and ProSAP2/Shank3 occurs within minutes, as measured by FRAP. Additionally, we could see a loss of Homer1 and to a lesser extent PSD-95 and NMDAR at PSDs after zinc depletion in young neurons or in the Shank1 knockdown condition. Given that Homer1 is a direct interaction partner of ProSAP/Shank family members, and furthermore that PSD-95 and NMDAR are found in layers close to or integrated into the cell membrane, one might conclude that a degradation of the PSD takes place, originating at the ProSAP/Shank scaffold, affecting direct interaction partners first and then gradually influencing layers of the PSD closer to the membrane. Additionally, the recovery of ProSAP2/Shank3 after CaEDTA induced zinc depletion by addition of $ZnCl_2$ takes place within the same time frame. Thus, one might reason that the sequence of events in synapse formation might happen in the opposite order. ProSAP1/Shank2 was previously identified as one of the first proteins found at forming synapses (Boeckers et al, 1999a) and that ProSAP1/Shank2 is highly enriched in growth cones of hippocampal primary neurons before synaptogenesis (Du et al, 1998). Upon formation of synaptic contacts, there is a striking change in the localization of ProSAP1/Shank2, becoming concentrated at the sites where PSDs are thought to form (Boeckers et al, 1999a). This early appearance at the differentiating postsynaptic membrane precedes the anchoring of PSD-95 and the NR1 subunit of the NMDA receptor (Boeckers et al, 1999a) and suggests that ProSAP1/Shank2 could be involved in initial steps of PSD assembly. Therefore, Zn^{2+} may be a key agent in the fast translation of synaptic plasticity into morphological alteration of synaptic contacts. Putative Zn^{2+} sources that could induce these changes might be represented by Zn^{2+} coreleased with neurotransmitter from presynaptic vesicles and entering the postsynapse through Ca^{2+}-permable channels (Koh and Choi, 1994; Sensi et al, 1999; Jia et al, 2002; Frederickson et al, 2005; Kay, 2006). Acute exposure of young rats to clioquinol, a zinc chelator, impairs long-term memory in the hippocampus by attenuation of dentate gyrus LTP, which may be associated with the transient lack of zinc release from zincergic neurons (Takeda et al, 2010).

Additionally, postsynaptic Zn^{2+} stores like metallothionins bind Zn^{2+} avidly and may release it rapidly in response to slight changes of postsynaptic redox states (Zhang et al, 2007). Independent of the physiological Zn^{2+} source, which remains to be identified, our results disclosed a striking interplay between Zn^{2+} ions and scaffolding molecules of the ProSAP/Shank family.

Materials and methods

Materials
$ZnCl_2$, the Zn^{2+} chelators CaEDTA and TPEN (N,N,N',N'-tetrakis (2-pyridylmethyl)ethylenediamine) and Zinquin ethyl ester were purchased from Sigma, Newport Green PDX acetoxymethyl ester from Invitrogen. Primary antibodies were purchased from Synaptic Systems (Gephyrin, Homer1, PSD-95, NMDAR1), Stressgen (Bassoon), Novus Biological (Shank1) and Chemicon (Map2). ProSAP1/Shank2 and ProSAP2/Shank3 antibodies have been described previously (Proepper et al, 2007). Secondary antibodies (Alexa) were from Invitrogen.

Hippocampal culture from rat brain
The preparation of hippocampal cultures was performed essentially as described by Goslin and Banker (1991), with some modifications

as detailed in Dresbach et al (2003). Cell culture experiments of hippocampal primary neurons from rat (embryonic day 18; E18) were performed as described previously (Seidenbecher et al, 1998; Dieterich et al, 2008). After preparation, the hippocampal neurons were seeded on poly-L-lysine (0.1 mg/ml; Sigma-Aldrich, Steinheim) glass coverslips in a 24-well plate at a density of 2×10^4 cells/well (for transfection and treatment of neurons) to 6×10^4 cells/well (for electron microscopy). Cells were grown in Neurobasal medium (Invitrogen), complemented with B27 supplement (Invitrogen), 0.5 mM L-Glutamine (Invitrogen) and 100 U/ml penicillin/streptomycin (Invitrogen) and maintained at 37°C in 5% CO_2.

All animal experiments were performed in compliance with the guidelines for the welfare of experimental animals issued by the Federal Government of Germany, the National Institutes of Health and the Max Planck Society.

Transfection and immunohistochemistry
Hippocampal cells were transfected at day 14 using OptiFect (Invitrogen). For a 24-well plate, 5 µl Optifect with 50 µl Neurobasal medium were incubated for 5 min at RT before mixing with 50 µl Neurobasal medium and 2 µg DNA per well and incubation for 30 min. Fluorescence images were obtained using an upright Axioscope microscope equipped with a Zeiss CCD camera (16 bits; 1280×1024 pixels per image) using the Axiovision software (Zeiss).

HeLa cells were transfected using Polyfect (Qiagen) transfection reagent. Cells were incubated with 15 µl PolyFect, 60 µl DMEM and 2 µg Plasmid-DNA overnight.

For immunofluorescence, the primary cultures were fixed with 4% paraformaldehyde/1.5% sucrose/PBS at 4°C for 20 min and processed for immunohistochemistry. After washing 3×5 min with $1 \times$ PBS at RT, blocking was performed with 0.5% cold fish gelatine (Sigma) and 0.1% Ovalbumin (Sigma)/$1 \times$ PBS for 30 min at RT and the cells were washed again 3 times 5 min with $1 \times$ PBS at RT, followed by the primary antibody at 4°C overnight. After a 3×5 min washing step with $1 \times$ PBS, incubation with the second antibody coupled to Alexa488, Alexa568 or Alexa647 for 1 h followed. The cells were washed again in $1 \times$ PBS for 10 min and 5 min with aqua bidest and mounted Mowiol with or without DAPI (for staining the nucleus) for fluorescence microscopy.

Expression constructs
The GKAP and PSD-95 constructs have been described previously (Bresler et al, 2001). The pEGFP (C1-3) vector system (Clontech, Palo Alto, CA) was used for ProSAP/Shank expression constructs. Mutated constructs have been described previously (Baron et al, 2006). For the gel-filtration experiments, two sets of ProSAP/Shank(SAM) expression constructs were created. The wild-type SAM domain of Shank1 (residues 2101–2362) and ProSAP2/Shank3 (residues 1674–1737) were cloned into the pMAL-c2x vector (New England Biolabs) using the SalI and HindIII sites to create MBP-Shank1(SAM) and MBP-ProSAP2/Shank3(SAM) constructs, respectively. In order to decrease loss of protein due to proteolysis between the MBP and SAM domains, a second pMAL-c2x-derived vector was designed in which the poly-N linker from SacI to SalI was replaced by the α-helical linker AEAAAKEAAAK (Nauli et al, 2007) These resulting constructs are referred to as MBP-AH-Shank1(SAM) and MBP-AH-Shank3(SAM).

RNAi oligonucleotides were purchased from MWG and cloned into a pSUPER vector. Three sequences were used for Shank1: 1189 nt from start: GATCCCC**AGAGACTCTTCAGGCATTA**TTCAAGA GA**TAATGCCTGAAGAGTCTCT**TTTTTGGAAA, 492 nt from start: GATCCCC**ACAGACCAACCTGGATGAG**TTCAAGAGA**CTCATCCAGGT TGGTCTGT**TTTTTGGAAA and 549 nt from start: GATCCCC**GAA GTTCCTTGAATATGTG**TTCAAGAGA**CACATATTCAAGGAACTTC**CTT TTTGGAAA. Two sequences were used for ProSAP1/Shank2: 32 nt from start: GATCCCC**TCGCCTGCTCCATGTTAAC**TTCAAGAGA**GTTA ACATGGAGCAGGCGA**TTTTTGGAAA and 406 nt from start: GATCC CC**TGCCTTCACCAAGAAGGAA**TTCAAGAGA**TTCCTTCTTGGTGAA GGCA**TTTTTGGAAA. ProSAP2/Shank3 target sequences were published earlier (Roussignol et al, 2005; Haeckel et al, 2008) and cloned into pSUPER. An RNAi-resistant Shank1 was generated using site-directed mutagenesis (QuickChange II XL site-directed mutagenesis; Stratagene) on a Shank1 clone fused to a myc-tag (Clontech pCMV-myc). Six point mutations were introduced into the RNAi target sequence leaving the amino-acid sequence unchanged (ACAAGGCAAA**A**AGG**C**T**TTT**TAGA**C**ATTACAC).

Western blotting

Proteins were separated by SDS–PAGE and blotted onto PVDF membrane. Immunoreactivity was visualized using HRP-conjugated secondary antibodies and the SuperSignal detection system (Pierce, Upland).

Treatment of hippocampal cells

For acute zinc substitution or depletion, hippocampal neurons were treated with 300 μM ZnCl₂ (Sigma) or the Zn chelators CaEDTA 10 mM and TPEN (N,N,N′,N′-tetrakis(2-pyridylmethyl)ethylenediamine) 10 μM (Sigma) at indicated concentrations and time. As a control, cells were treated with Mannitol (Sigma), CaCl₂ and MgCl₂ (Sigma). All control experiments showed that the described effects were Zn specific and not dependent upon osmolarity of the medium (data not shown). Growth media were supplemented with zinc chelators or ZnCl₂ and incubated at 37°C, 5% CO₂. After incubation, cells were washed three times with PBS and fixed for immunocytochemistry or stained with Zinquin or Newport Green.

Synapse measurements

Pictures and were taken from neuronal synapses of hippocampal neurons with an upright Axioscope microscope equipped with a Zeiss CCD camera. The number, diameter and area of the synapses was measured using ImageJ 1.44d for Mac and Axiovision Software.

Statistical analysis in this paper was performed using Microsoft Excel for Mac and tested for significance using t-tests, P-values < 0.05 were stated as significant ($< 0.05*$; $< 0.01**$; $< 0.001***$). For evaluation, either fluorescent puncta along dendrites within the field of view were counted and the amount of monofluorescent (i.e. 'Homer only') and double-fluorescent (i.e. 'Bassoon/Homer') signals was compared with the total amount of fluorescent puncta or fluorescent puncta along primary and secondary dendrites were counted and related to the measured dendrite length.

For the evaluation of EM data, values were tested for significance using Kruskal–Wallis test, again P-values < 0.05 were stated as significant ($< 0.05*$; $< 0.01**$; $< 0.001***$). PSDs with a depth of > 30 nm were counted as 'strong' as wells as with an area of > 6000 nm².

Zinc staining

Zinquin ethyl ester was stored as a 5-M stock solution in DMSO at -20°C. Cryosections from rat brain or hippocampal neurons in cultures were stained with Zinquin ethyl ester. For cell culture neurons, growth medium was discarded and the cells were washed three times with HBBS. Coverslips were incubated with a solution of 25 μM Zinquin ethyl ester in HBSS for 40 min at 37°C (Coyle et al, 1994). Zinquin ethyl ester and Newport Green PDX-Ac are cell permeant and the ester is cleaved by intracellular esterases to become a cell impermeant zinc indicator. For NG-AC staining, cells in PBS were exposed 45 min at 37°C to 50 μM NG-Ac containing 1.5 μl/ml Pluronic F-127 (Sigma) to enhance cell penetration. Afterwards, the probes were washed three times with PBS (Lukowiak et al, 2001).

Protein purification

The MBP constructs were transformed into ARI814 cells (Schatz et al, 1996) and grown at 37°C in LB media supplemented with 100 μg/ml Ampicillin until the cell density reached an OD₆₀₀ of 0.8. Cells were induced with 1 mM isopropyl-b-D-galactopyranoside and incubated at 37°C for an additional 2 h at which point they were harvested by centrifugation. In all, 40 g of the cell pellet was resuspended in 140 ml of 20 mM Tris (pH 7.5)/300 mM NaCl/1 mMTCEP/0.5 mM PMSF/lysozyme (1 mg/ml)/DnaseI (10 μg/ml)/5 mM MgCl₂ and eight tablets of Complete Protease Inhibitor (Roche). The cells were lysed by sonication and the lysate was centrifuged at 27 000 g for 45 min. The supernatant was incubated with 50 ml Amylose resin (New England Biolabs) for 1 h at 4°C. The resin was poured into a column and washed with seven column volumes of 20 mM Tris (pH 7.5)/300 mM NaCl/1 mM TCEP and protein was eluted with 20 mM Tris (pH 7.5)/300 mM NaCl/1 mM TCEP/10 mM Maltose. The eluted protein was then applied to a 5-ml IMAC-HP column (GE Biosciences) charged with zinc acetate and the bound protein was eluted with 15 ml of 20 mM Tris (pH 7.5)/300 mM NaCl/1 mM TCEP/400 mM imidazole. The protein was dialyzed at 4°C for 4 h against 2 l of 20 mM Tris (pH 7.5)/500 mM NaCl and transferred to 2 l of the same buffer overnight. Dialyzed

protein was concentrated using an Amicon Ultra centrifugal filter concentrator unit (Millipore) to a concentration of 10 μM.

Gel filtration-zinquin assay

In all, 650 μl of 10 μM MBP-Shank1(SAM) and MBP-ProSAP2/Shank3(SAM) protein in 20 mM Tris (pH 7.5)/500 mM NaCl was incubated with 10 μM zinc acetate for 30 min at room temperature. Protein solutions were then centrifuged for 10 min at 16 000 g to remove the precipitated protein from the soluble protein. The concentration of the soluble fraction was adjusted to yield polymer peaks with an OD of about 11 mAU in order to compare peaks with equivalent protein concentration despite the fact that a greater amount of Shank3 protein was lost to precipitation after zinc addition. In all, 500 μl were loaded onto a Superdex200-10/300GL gel-filtration column (Amersham Biosciences) at 0.5 ml/min and 250 μl fractions were collected. A measure of 5 μl of 5 mM Zinquin ethyl ester (Sigma) dissolved in DMSO was added to 200 μl of each fraction and incubated for 20 min at room temperature. Zinquin fluorescence was monitored in 96-well clear bottom, black-sided plates (Nunc) on a Molecular Devices Spectramax M5 platereader using an excitation wavelength of 368 nm, an emission wavelength of 510 nm, and a cutoff filter of 495 nm.

Zinc-precipitated protein zinquin assay

In all, 650 μl of 10 μM MBP-AH-Shank1(SAM) and MBP-AH-Shank3(SAM) protein in 20 mM Tris (pH 7.5)/500 mM NaCl was subjected to zinc incubation, as described above. The insoluble, zinc-precipitated fraction of protein was washed with three successive rounds of resuspension in 1 ml of 20 mM Tris (pH 7.5)/500 mM NaCl. Washed precipitate was resuspended in 220 μl buffer. A 10-μl aliquot of protein was removed to ascertain the protein concentration by adding urea to 6 M and measuring the absorbance at 280 nm. The precipitate suspensions were then adjusted to roughly 5 μM and the final suspension concentration was confirmed again by aliquot denaturation. In all, 200 μl of suspension was incubated with 10 μM Zinquin ethyl ester for 20 min and assayed in a microplate as described above. The assay was repeated in triplicate and the background fluorescence was estimated using a control zinc incubation with MBP for which no precipitate was observed. Total sample fluorescence, corrected for background fluorescence, was normalized to the total amount of protein present in the sample. The results of three independent assays with each construct were averaged.

Metal occupancy of the ProSAP2/Shank3 SAM domain purified from E. coli

Samples were analysed at the UCLA, Department of Chemistry and Biochemistry Elemental Analysis Facility using an Agilent 7500ce Quadrupole ICP-MS equipped with an H₂/He/Xe Octapole Reaction/Collision Cell. Instrument parameters were as follows: 1550 RF power, 1.05 l/min carrier gas, 0.1 r.p.s. nebulizer pump, 2°C spray chamber temperature, 4 and 5 ml/min of H₂ and He, respectively, were used when the analysis required interference removal by the collision cell. To the protein samples, 200 μl of Ultrapure Nitric Acid (Optima, Fisher, CA) was added. The samples were heated to 90°C on a 48-well digestion block (ModBlock, CPI International, Santa Rosa, CA), with a digital temperature controller and allowed to digest until no particulate or colour change was observed. The temperature was then raised to 110°C and the samples were allowed to evaporate to ∼50 μl. After cooling, the samples were diluted to 6 ml with ultra pure water and the final nitric acid concentration was adjusted to 2%. Calibration solutions were diluted from a 100 p.p.m. multi-element stock solution (CPI International, Santa Rosa, CA) and scandium at a final concentration of 500 p.p.b. was added to all samples and calibration standards.

Transmission electron microscopy

Cells were fixed at DIV 14 in 0.1 M phosphate buffer pH 7.3, containing 2.5% glutaraldehyde, 1% sucrose and were osmicated for 1 h in 2% OsO₄. Then they were dehydrated in graded series of ethanol, contrasted in 2% uranyl acetate and embedded in epoxy resin (Fluka, Germany) at 60°C. Thin sections of 70–80 nm were cut with a diamond knife on a Reichert ultramicrotome and collected on 300 mesh grids. The sections were contrasted with 0.3% lead citrate for 1 min and analysed on a transmission electron microscope EM 10 (Zeiss) at 80 kV. Electron micrographs were taken at random positions at a magnification of × 5000.

Conflict of interest

The authors declare that they have no conflict of interest.

References

Bailey CH, Kandel ER (1993) Structural changes accompanying memory storage. *Annu Rev Physiol* **55:** 397–426

Baron MK, Boeckers TM, Vaida B, Faham S, Gingery M, Sawaya MR, Salyer D, Gundelfinger ED, Bowie JU (2006) An architectural framework that may lie at the core of the postsynaptic density. *Science* **311:** 531–535

Berkel S, Marshall CR, Weiss B, Howe J, Roeth R, Moog U, Endris V, Roberts W, Szatmari P, Pinto D, Bonin M, Riess A, Engels H, Sprengel R, Scherer SW, Rappold GA (2010) Mutations in the SHANK2 synaptic scaffolding gene in autism spectrum disorder and mental retardation. *Nat Genet* **42:** 489–491

Boeckers TM, Bockmann J, Kreutz MR, Gundelfinger ED (2002) ProSAP/Shank proteins—a family of higher order organizing molecules of the postsynaptic density with an emerging role in human neurological disease. *J Neurochem* **81:** 903–910

Boeckers TM, Kreutz MR, Winter C, Zuschratter W, Smalla KH, Sanmarti-Vila L, Wex H, Langnaese K, Bockmann J, Garner CC, Gundelfinger ED (1999a) Proline-rich synapse-associated protein- 1/cortactin binding protein 1 (ProSAP1/CortBP1) is a PDZ-do- main protein highly enriched in the postsynaptic density. *J Neurosci* **19:** 6506–6518

Boeckers TM, Liedtke T, Spilker C, Dresbach T, Bockmann J, Kreutz MR, Gundelfinger ED (2005) C-terminal synaptic targeting ele- ments for postsynaptic density proteins ProSAP1/Shank2 and ProSAP2/Shank3. *J Neurochem* **92:** 519–524

Boeckers TM, Winter C, Smalla KH, Kreutz MR, Bockmann J, Seidenbecher C, Garner CC, Gundelfinger ED (1999b) Proline- rich synapse-associated proteins ProSAP1 and ProSAP2 interact with synaptic proteins of the SAPAP/GKAP family. *Biochem Biophys Res Commun* **264:** 247–252

Bresler T, Ramati Y, Zamorano PL, Zhai R, Garner CC, Ziv NE (2001) The dynamics of SAP90/PSD-95 recruitment to new synaptic junctions. *Mol Cell Neurosci* **18:** 149–167

Bresler T, Shapira M, Boeckers T, Dresbach T, Futter M, Garner CC, Rosenblum K, Gundelfinger ED, Ziv NE (2004) Postsynaptic density assembly is fundamentally different from presynaptic active zone assembly. *J Neurosci* **24:** 1507–1520

Coyle P, Zalewski PD, Philcox JC, Forbes IJ, Ward AD, Lincoln SF, Mahadevan I, Rofe AM (1994) Measurement of zinc in hepato- cytes by using a fluorescent probe, zinquin: relationship to metallothionein and intracellular zinc. *Biochem J* **303:** 781–786

Dieterich DC, Karpova A, Mikhaylova M, Zdobnova I, König I, Landwehr M, Kreutz M, Smalla KH, Richter K, Landgraf P, Reissner C, Boeckers TM, Zuschratter W, Spilker C, Seidenbecher CI, Garner CC, Gundelfinger ED, Kreutz MR (2008) Caldendrin-Jacob: a protein liaison that couples NMDA receptor signalling to the nucleus. *PLoS Biol* **6:** e34

Dresbach T, Hempelmann A, Spilker C, tom Dieck S, Altrock WD, Zuschratter W, Garner CC, Gundelfinger ED (2003) Functional regions of the presynaptic cytomatrix protein bassoon: signifi- cance for synaptic targeting and cytomatrix anchoring. *Cell Neurosci* **23:** 279–291

Du Y, Weed SA, Wen-Cheng X, Marshall TD, Parsons TJ (1998) Identification of a novel cortactin SH3 domain-binding protein and its localization to growth cones of cultured neurons. *Mol Cell Biol* **18:** 5838–5851

Durand CM, Betancur C, Boeckers TM, Bockmann J, Chaste P, Fauchereau F, Nygren G, Rastam M, Gillberg IC, Anckarsäter H, Sponheim E, Goubran-Botros H, Delorme R, Chabane N, Mouren-Simeoni MC, de Mas P, Bieth E, Rogé B, Héron D, Burglen L *et al* (2007) Mutations in the gene encoding the synaptic scaffolding protein SHANK3 are associated with autism spectrum disorders. *Nat Genet* **39:** 25–27

Fahrni CJ, O'Halloran TV (1999) Aqueous coordination chemistry of quinoline-based fluorescence probes for the biological chemistry of zinc. *J Am Chem Soc* **121:** 11448

Fernandez F, Morishita W, Zuniga E, Nguyen J, Blank M, Malenka RC, Garner CC (2007) Pharmacotherapy for cognitive impairment in a mouse model of Down syndrome. *Nat Neurosci* **10:** 411–413

Frederickson CJ, Koh JY, Bush AI (2005) The neurobiology of zinc in health and disease. *Nat Rev Neurosci* **6:** 449–462

Gauthier J, Champagne N, Lafrenière RG, Xiong L, Spiegelman D, Brustein E, Lapointe M, Peng H, Côté M, Noreau A, Hamdan FF, Addington AM, Rapoport JL, Delisi LE, Krebs MO, Joober R, Fathalli F, Mouaffak F, Haghighi AP, Néri C *et al* (2010) *De novo* mutations in the gene encoding the synaptic scaffolding protein SHANK3 in patients ascertained for schizophrenia. *Proc Natl Acad Sci USA* **107:** 7863–7868

Gerrow K, Romorini S, Nabi SM, Colicos MA, Sala C, El-Husseini A (2006) A preformed complex of postsynaptic proteins is involved in excitatory synapse development. *Neuron* **49:** 547–562

Golub MS, Keen CL, Gershwin ME, Hendrickx AG (1995) Developmental zinc deficiency and behavior. *J Nutr* **125:** 2263–2271

Gong Y, Lippa CF, Zhu J, Lin Q, Rosso AL (2009) Disruption of glutamate receptors at Shank-postsynaptic platform in Alzheimer's disease. *Brain Res* **1292:** 191–198

Goslin K, Banker G (1991) Rat hippocampal neurons in low density culture. In *Culturing Nerve Cells*, Banker G, Goslin K (eds), pp 251–281. Cambridge, MA: MIT Press

Grabrucker A, Vaida B, Bockmann J, Boeckers TM (2009a) Synaptogenesis of hippocampal neurons in primary cell culture. *Cell Tissue Res* **338:** 333–341

Grabrucker AM, Vaida B, Bockmann J, Boeckers TM (2009b) Efficient targeting of proteins to post-synaptic densities of excita- tory synapses using a novel pSDTarget vector system. *J Neurosci Methods* **181:** 227–234

Gray EG (1959) Axo-somatic and axo-dendritic synapses of the cerebral cortex: an electron microscope study. *J Anat* **93:** 420–433

Gundelfinger ED, Boeckers TM, Baron MK, Bowie JU (2006) A role for zinc in postsynaptic density asSAMbly and plasticity? *Trends Biochem Sci* **31:** 366–373

Haeckel A, Ahuja R, Gundelfinger ED, Qualmann B, Kessels MM (2008) The actin-binding protein Abp1 controls dendritic spine morphology and is important for spine head and synapse forma- tion. *J Neurosci* **28:** 10031–10044

Harris KM, Kater SB (1994) Dendritic spines: cellular specializations imparting both stability and flexibility to synaptic function. *Annu Rev Neurosci* **17:** 341–371

Hayashi MK, Tang C, Verpelli C, Narayanan R, Stearns MH, Xu RM, Li H, Sala C, Hayashi Y (2009) The postsynaptic density proteins Homer and Shank form a polymeric network structure. *Cell* **137:** 159–171

Horner CH (1993) Plasticity of the dendritic spine. *Prog Neurobiol* **41:** 281–321

Huang YZ, Pan E, Xiong ZQ, McNamara JO (2008) Zinc-mediated transactivation of TrkB potentiates the hippocampal mossy fiber- CA3 pyramid synapse. *Neuron* **57:** 546–558

Hung AY, Futai K, Sala C, Valtschanoff JG, Ryu J, Woodworth MA, Kidd FL, Sung CC, Miyakawa T, Bear MF, Weinberg RJ, Sheng M (2008) Smaller dendritic spines, weaker synaptic transmission, but enhanced spatial learning in mice lacking Shank1. *J Neurosci* **28:** 1697–1708

Jan HH, Chen IT, Tsai YY, Chang YC (2002) Structural role of zinc ions bound to postsynaptic densities. *J Neurochem* **83:** 525–534

Jia Y, Jeng JM, Sensi SL, Weiss JH (2002) Zn^{2+} currents are mediated by calcium-permeable AMPA/kainate channels in cul- tured murine hippocampal neurones. *J Physiol* **543:** 35–48

Kay AR (2006) Imaging synaptic zinc: promises and perils. *Trends Neurosci* **29:** 200–206

Koh JY, Choi DW (1994) Zinc toxicity on cultured cortical neurons: involvement of *N*-methyl-D-aspartate receptors. *Neuroscience* **60:** 1049–1057

Kim E, Sheng M (2004) PDZ domain proteins of synapses. *Nat Rev Neurosci* **5:** 771–781

Li Y, Hough CJ, Frederickson CJ, Sarvey JM (2001) Induction of mossy fiber→Ca3 long-term potentiation requires translocation of synaptically released Zn^{2+}. *J Neurosci* **21:** 8015–8025

Lim S, Naisbitt S, Yoon J, Hwang JI, Suh PG, Sheng M, Kim E (1999) Characterization of the Shank family of synaptic proteins. Multiple genes, alternative splicing, and differential expression in brain and development. *J Biol Chem* **274:** 29510–29518

Lukowiak B, Vandewalle B, Riachy R, Kerr-Conte J, Gmyr V, Belaich S, Lefebvre J, Pattou F (2001) Identification and purification of functional human beta-cells by a new specific zinc-fluorescent probe. *J Histochem Cytochem* **49:** 519–528

Naisbitt S, Kim E, Tu JC, Xiao B, Sala C, Valtschanoff J, Weinberg RJ, Worley PF, Sheng M (1999) Shank, a novel family of postsynaptic density proteins that binds to the NMDA receptor/PSD-95/GKAP complex and cortactin. *Neuron* **23:** 569–582

Nauli S, Farr S, Lee YJ, Kim HY, Faham S, Bowie JU (2007) Polymer-driven crystallization. *Protein Sci* **16:** 2542–2551

Palmiter RD, Cole TB, Quaife CJ, Findley SD (1996) ZnT-3, a putative transporter of zinc into synaptic vesicles. *Proc Natl Acad Sci USA* **93:** 14934–14939

Petralia RS, Sans N, Wang YX, Wenthold RJ (2005) Ontogeny of postsynaptic density proteins at glutamatergic synapses. *Mol Cell Neurosci* **29:** 436–452

Pham E, Crews L, Ubhi K, Hansen L, Adame A, Cartier A, Salmon D, Galasko D, Michael S, Savas JN, Yates JR, Glabe C, Masliah E (2010) Progressive accumulation of amyloid-beta oligomers in Alzheimer's disease and in amyloid precursor protein transgenic mice is accompanied by selective alterations in synaptic scaffold proteins. *FEBS J* **277:** 3051–3067

Proepper C, Johannsen S, Liebau S, Dahl J, Vaida B, Bockmann J, Kreutz MR, Gundelfinger ED, Boeckers TM (2007) Abelson interacting protein 1 (Abi-1) is essential for dendrite morphogenesis and synapse formation. *EMBO J* **26:** 1397–1409

Romorini S, Piccoli G, Jiang M, Grossano P, Tonna N, Passafaro M, Zhang M, Sala C (2004) A functional role of postsynaptic density-95-guanylate kinase-associated protein complex in regulating Shank assembly and stability to synapses. *J Neurosci* **24:** 9391–9404

Roselli F, Hutzler P, Wegerich Y, Livrea P, Almeida OF (2009) Disassembly of shank and homer synaptic clusters is driven by soluble beta-amyloid(1–40) through divergent NMDAR-dependent signalling pathways. *PloS One* **4:** e6011

Rostaing P, Real E, Siksou L, Lechaire JP, Boudier T, Boeckers TM, Gertler F, Gundelfinger ED, Triller A, Marty S (2006) Analysis of synaptic ultrastructure without fixative using high-pressure freezing and tomography. *Eur J Neurosci* **24:** 3463–3474

Roussignol G, Ango F, Romorini S, Tu JC, Sala C, Worley PF, Bockaert J, Fagni L (2005) Shank expression is sufficient to induce functional dendritic spine synapses in aspiny neurons. *J Neurosci* **25:** 3560–3570

Rubenstein JL, Merzenich MM (2003) Model of autism: increased ratio of excitation/inhibition in key neural systems. *Genes Brain Behav* **2:** 255–267

Sala C, Piëch V, Wilson NR, Passafaro M, Liu G, Sheng M (2001) Regulation of dendritic spine morphology and synaptic function by Shank and Homer. *Neuron* **31:** 115–130

Schatz PJ, Cull MG, Martin EL, Gates CM (1996) Screening of peptide libraries linked to lac repressor. *Methods Enzymol* **267:** 171–191

Seidenbecher CI, Langnaese K, Sanmarti-Vila L, Boeckers TM, Smalla KH, Sabel BA, Garner CC, Gundelfinger ED, Kreutz MR (1998) Caldendrin, a novel neuronal calcium-binding protein confined to the somato-dendritic compartment. *J Biol Chem* **14:** 21324–21331

Sensi SL, Yin HZ, Carriedo SG, Rao SS, Weiss JH (1999) Preferential Zn^{2+} influx through Ca^{2+}-permeable AMPA/kainate channels triggers prolonged mitochondrial superoxide production. *Proc Natl Acad Sci USA* **96:** 2414–2419

Sheng M, Kim E (2000) The Shank family of scaffold proteins. *J Cell Sci* **113:** 1851–1856

Singer HS, Minzer K (2003) Neurobiology of Tourette's syndrome: concepts of neuroanatomic localization and neurochemical abnormalities. *Brain Dev* **25:** 70–84

Takeda A (2000) Movement of zinc and its functional significance in the brain. *Brain Res Brain Res Rev* **34:** 137–148

Takeda A, Takada S, Ando M, Itagaki K, Tamano H, Suzuki M, Iwaki H, Oku N (2010) Impairment of recognition memory and hippocampal long-term potentiation after acute exposure to clioquinol. *Neuroscience* **171:** 443–450

Wassef A, Baker J, Kochan LD (2003) GABA and schizophrenia: a review of basic science and clinical studies. *J Clin Psychopharmacol* **23:** 601–640

Wenzel HJ, Cole TB, Born DE, Schwartzkroin PA, Palmiter RD (1997) Ultrastructural localization of zinc transporter-3 (ZnT-3) to synaptic vesicle membranes within mossy fiber boutons in the hippocampus of mouse and monkey. *Proc Natl Acad Sci USA* **94:** 12676–12681

Wigstrom H, Gustafsson B (1983) Facilitated induction of hippocampal long-lasting potentiation during blockade of inhibition. *Nature* **301:** 603–604

Zhang Y, Aizenman E, DeFranco DB, Rosenberg PA (2007) Intracellular zinc release, 12-lipoxygenase activation and MAPK dependent neuronal and oligodendroglial death. *Mol Med* **13:** 350–355